The effect of high pressure on antiferromagnetic correlations in the Kondo semimetal CeNiSn

1996 J. Phys.: Condens. Matter 8 8183

(http://iopscience.iop.org/0953-8984/8/43/014)

J. Phys.: Condens. Matter **8** (1996) 8183–8189. Printed in the UK

The effect of high pressure on antiferromagnetic correlations in the Kondo semimetal CeNiSn

Taku J Sato†‖, Hiroaki Kadowaki†¶, Toshiro Takabatake‡+, Hironobu Fujii‡ and Yosikazu Isikawa§

† Institute for Solid State Physics, University of Tokyo, Roppongi, Minato-ku, Tokyo 106, Japan
‡ Faculty of Integrated Arts and Sciences, Hiroshima University, Higashi-Hiroshima 739, Japan
§ Faculty of Science, Toyama University, Toyama 930, Japan

Received 8 May 1996, in final form 27 August 1996

Abstract. Magnetic excitation spectra of the Kondo semimetal CeNiSn have been studied by neutron scattering under hydrostatic pressure up to 11 kbar. The inelastic peak at $\hbar\omega = 4$ meV has been observed at the ambient pressure below $T_{coh} = 20$ K and is regarded as a dynamic antiferromagnetic correlation. As pressure is applied, the 4 meV peak shifts to a higher-energy region and becomes weak. Since the pseudogap is known to be suppressed under high pressure, this result strongly suggests that the antiferromagnetic correlation is closely related to pseudogap formation.

1. Introduction

An energy gap at the Fermi level is formed at low temperatures in certain heavy-fermion or valence-fluctuation compounds, such as CeNiSn [1], CeRhSb [2], $Ce_3Bi_4Pt_3$ [3], SmB_6 [4] and YbB_{12} [5]. Among them, CeNiSn, which crystallizes in the ϵ-TiNiSi structure [6], attracts special attention since it is situated close to a boundary of the insulating and metallic regions [1]. Various physical properties, such as the specific heat [7], $1/T_1$ of NMR [8] and so on, show the gap opening at the Fermi level below $T_\Delta \simeq 6$ K. This gap is very narrow and incomplete: there remains a finite density of states at the Fermi level [8, 9]. In addition, the gap is anisotropic and closes at least along the a-axis [10]. Thus the gap is called a 'pseudogap'.

A key to understanding the origin of the pseudogap formation is believed to lie in the antiferromagnetic correlations, i.e., coherence in the Ce lattice, which develop below the coherence temperature $T_{coh} = 20$ K. The development of the antiferromagnetic correlations was first suggested from the static susceptibility [1], and was most clearly observed in the neutron inelastic-excitation spectra [11, 12]. In the spectra, they appear as peaks at $\hbar\omega = 2$ meV and $\boldsymbol{Q} = (0, 0, 1)$ or $(0, 1, 0)$ [11, 12], and at $\hbar\omega = 4$ meV and $\boldsymbol{Q} = (Q_a, \frac{1}{2} + n, Q_c)$, where Q_a and Q_c are arbitrary and n is an integer [12]. From their $\boldsymbol{Q}$-dependence, the 2 and 4 meV peaks can be regarded as three-dimensional and quasi-one-dimensional dynamic antiferromagnetic correlations, respectively.

The narrow and anisotropic pseudogap is easily suppressed by applying a high magnetic field (∼10 T) [1], or partly substituting constituent materials, for instance 3% Co for Ni

‖ Present address: National Research Institute for Metals, Sengen, Tsukuba, Ibaraki 305, Japan.
¶ Present address: Department of Physics, Tokyo Metropolitan University, Hachioji-shi, Tokyo 192-03, Japan.
+ Present address: Faculty of Science, Hiroshima University, Higashi-Hiroshima 739, Japan.

0953-8984/96/438183+07$19.50

[13]. To reveal a relationship between the pseudogap formation and antiferromagnetic correlations, two neutron inelastic-scattering experiments have been performed so far on gap-suppressed samples: $CeNi_{0.9}Co_{0.1}Sn$ [14] and CeNiSn in the high magnetic field of 10 T [15]. In both cases, the antiferromagnetic correlations are suppressed along with the collapse of the pseudogap, suggesting a close relationship between them.

Suppression of the pseudogap has also been observed under high pressure. The electrical resistivity measurement by Kurisu *et al* [16] shows that the upturn of the resistivity below T_Δ disappears under a hydrostatic pressure of about 12 kbar, indicating pseudogap suppression. Suppression is also seen in the Hall coefficient measurement [17], which shows the increase of carrier number under pressure. The electrical resistivity further suggests that CeNiSn becomes valence fluctuating under high pressure from the moderately heavy-fermion system under ambient pressure.

In this study, we have performed neutron inelastic-scattering experiments under hydrostatic pressure up to 11 kbar. The hydrostatic pressure does not introduce randomness in the lattice, and it mainly changes the strength of c–f hybridization. Further, it will not break the symmetry in the spin space, while the magnetic field does. Thus high-pressure neutron scattering seems to be the most promising experimental technique for revealing the relationship between antiferromagnetic correlations and pseudogap formation.

2. Experimental procedure

A single-crystalline sample of CeNiSn was grown by the Czochralski method [18]. The volume of the single crystal was 0.16 cm^3. The neutron scattering experiments were performed on the triple-axis spectrometer ISSP GPTAS installed at JRR-3M JAERI (Tokai). Pyrolytic graphite (002) reflections were used for the vertically focusing monochromator and analyser. The spectrometer was operated with final energy fixed to 13.7 meV. Higher-order neutrons were removed by a pyrolytic graphite filter. Collimations of 30′–40′–40′–80′ were employed. This configuration yields an energy resolution of 0.9 meV at the elastic position in full width at half-maximum.

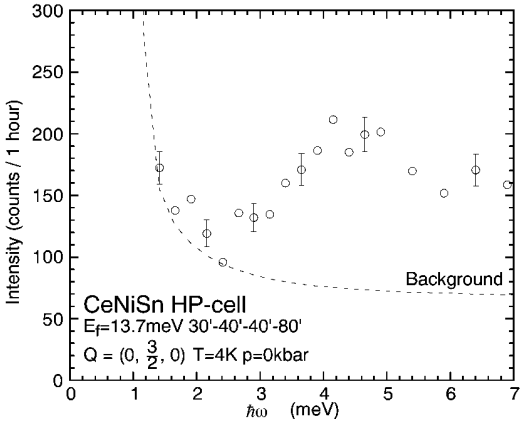

Figure 1. A constant-$\boldsymbol{Q}$ scan at $\boldsymbol{Q} = (0, \frac{3}{2}, 0)$ and $T = 4$ K, and at the ambient pressure. The raw data are shown. The dotted line stands for the background.

Hydrostatic pressure up to 11 kbar was applied to the sample using a clamping-type high-pressure cell for neutron scattering [19]. The crystal was mounted in the cell with

the b-axis in the scattering plane so as to measure the scattering on the $\boldsymbol{b}^*$-axis. The other direction in the scattering plane was not completely determined, but was almost parallel to the [201] direction with an ambiguity of $\pm 10^\circ$. The pressure was generated at room temperature using Fluorinert as the pressure-transmitting fluid. The cell was mounted in a closed-cycle ^{4}He refrigerator and cooled down to 4 K. Since the generated pressure slightly decreases at low temperatures, we determined the pressure by measuring the lattice constant of a NaCl single crystal, which was mounted in the cell together with the CeNiSn [19].

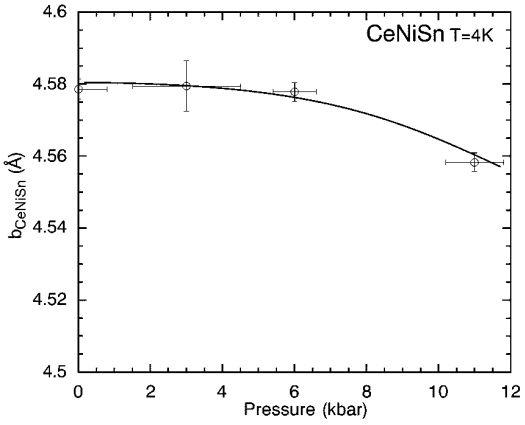

Figure 2. The pressure dependence of the lattice constant b of CeNiSn, observed at $T = 4$ K. The solid line is a guide to the eye.

A typical result of a constant-$\boldsymbol{Q}$ scan in CeNiSn in the high-pressure cell is shown in figure 1. The spectrum was observed at ambient pressure, and at $\boldsymbol{Q} = (0, \frac{3}{2}, 0)$ and $T = 4$ K. In addition to the inelastic-excitation peak at $\hbar\omega = 4$ meV, there appears a large background, which originates from the high-pressure cell and Fluorinert. The large background prevented us from observing the 2 meV excitation peak, which is of very low intensity [11, 12]. Thus we only investigated the pressure dependence of the 4 meV peak. Spectra shown in the following section are corrected for background and absorption. They were scaled to absolute units of cross-section by comparing the peak intensity of the spectrum at the ambient pressure observed in the present study with that in an earlier report [12]. They are given as the scattering function $S(\boldsymbol{Q}, \hbar\omega) = (k_i/k_f)(\mathrm{d}^2\sigma/\mathrm{d}\Omega\ \mathrm{d}E_f)$.

3. Results and discussion

We first investigated the pressure dependence of the lattice constant of CeNiSn. Figure 2 shows the variation of the lattice constant b of CeNiSn measured at $T = 4$ K. The lattice constant b decreases with pressure; however, at low pressure ($p < 6$ kbar) the variation is very small.

The inelastic-excitation spectra at $\boldsymbol{Q} = (0, \frac{3}{2}, 0)$ and $T = 4$ K, and at the pressures p = 0, 3, 6 and 11 kbar, are shown in figure 3. The spectra at the higher temperatures $T = 25$ K ($p = 0$ kbar) and 50 K ($p = 6$ kbar) are also shown in the figure. At ambient pressure, we confirmed the clear inelastic peak at $\hbar\omega = 4$ meV. Since the profile of the spectrum is the same as that observed in [12], we conclude that there is no spurious peak from the high-pressure cell and Fluorinert. The result that the peak disappears at $T = 25$ K $> T_{\mathrm{coh}}$ further confirms the magnetic nature of the peak. As the pressure becomes larger, the intensity of

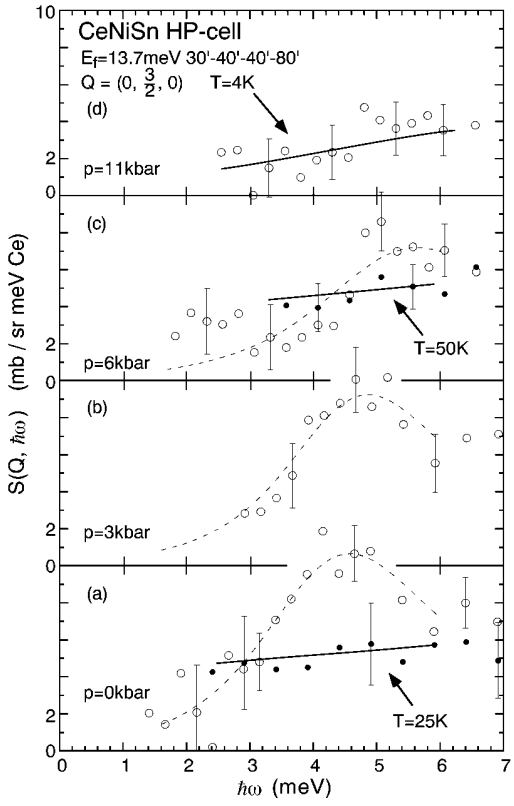

Figure 3. Constant-$\boldsymbol{Q}$ scans at $\boldsymbol{Q} = (0, \frac{3}{2}, 0)$, and at the pressures $p = 0, 3, 6$ and 11 kbar. The open circles stand for data taken at $T = 4$ K, whereas the closed circles for $p = 0$ and 6 kbar stand for data taken at $T = 25$ and 50 K, respectively. The dotted and solid lines denote the resolution-convoluted approximate function of equation (1) and a guide to the eye, respectively.

the peak becomes smaller, and the peak position shifts to the higher-energy region. Below 6 kbar, however, the 4 meV peak could be observed. At $p = 11$ kbar, the spectrum becomes flat and shows no peak below 6 meV.

To parametrize the pressure dependence of the peak profile, we tried to fit the inelastic-excitation spectra with the following inelastic Lorentzian function:

$$S(\boldsymbol{Q}, \overline{h}\omega) \propto \frac{\operatorname{Im}\chi(\boldsymbol{Q}, \overline{h}\omega)}{1 - \mathrm{e}^{-\beta\overline{h}\omega}} \propto \frac{\overline{h}\omega}{1 - \mathrm{e}^{-\beta\overline{h}\omega}} \left(\frac{\Gamma}{(\overline{h}\omega + \overline{h}\omega_0)^2 + \Gamma^2} + \frac{\Gamma}{(\overline{h}\omega - \overline{h}\omega_0)^2 + \Gamma^2} \right) \qquad (1)$$

where β is defined as $\beta = 1/k_{\mathrm{B}}T$. This function was found to reproduce the peak profile at the ambient pressure [12]. Since there is phonon contamination above 6 meV [12], the energy region used for the fit was limited to $2 < \overline{h}\omega < 6$ meV. We performed the fitting with the spectra for $p \leqslant 6$ kbar, since the spectrum for $p = 11$ kbar shows no peak below 6 meV. In the fitting, the trial function (1) was convoluted with the spectrometer resolution by using the FIT3AX program developed at Brookhaven National Laboratory, which is based on the instrumental resolution function of the triple-axis spectrometer deduced by Chesser and Axe [20]. The resulting pressure dependences of the peak energy $\overline{h}\omega_0$, the width Γ and the peak intensity $S_{\max} = S(\boldsymbol{Q}, \overline{h}\omega_0)$ are shown in figures 4(a), 4(b) and 4(c), respectively. The peak energy $\overline{h}\omega_0$ increases and the peak intensity $S_{\max}$ decreases almost linearly with p, whereas

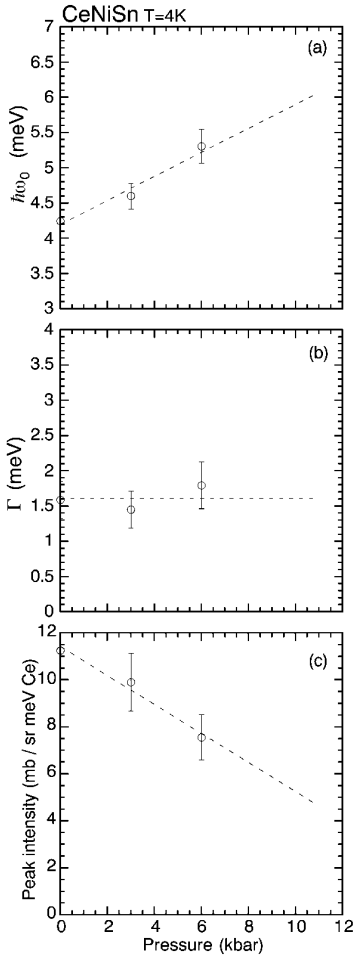

Figure 4. The pressure dependence of (a) the peak energy $\overline{h}\omega_0$, (b) the width Γ and (c) the peak intensity $S_{\max} = S(\boldsymbol{Q}, \overline{h}\omega_0)$ at $T = 4$ K. $\overline{h}\omega_0$, Γ and $S_{\max}$ were determined by fitting the spectra in figure 3 with the approximate function of equation (1). The dotted lines are the approximate functions for the pressure dependence, which are $\overline{h}\omega_0 = 4.2 + 0.17p$, $\Gamma = 1.6$ and $S_{\max} = 11.4 - 0.62p$.

the width Γ is rather independent of pressure. The pressure dependence of $\overline{h}\omega_0$ and $S_{\max}$ can be approximated as $\overline{h}\omega_0 = 4.2 + 0.17p$ and $S_{\max} = 11.4 - 0.62p$, respectively. By extrapolating the pressure dependence of $\overline{h}\omega_0$ and $S_{\max}$, we suggest that the 4 meV peak shifts to $\overline{h}\omega > 6$ meV and also becomes weak at $p = 11$ kbar. This may be the reason that the spectrum below 6 meV is flat and featureless as shown in figure 3(d). Since both the inelastic-excitation peak and the pseudogap in the resistivity disappear under high pressure, it is strongly suggested that the antiferromagnetic correlation and the pseudogap formation are closely related to each other.

Neutron inelastic excitation allows one to observe the magnetic fluctuations of 4f moments, but those of the conduction electrons are barely discernible, because of the difference of their form factors. Thus we interpreted the inelastic-excitation peaks as dynamic antiferromagnetic correlations among Ce 4f moments. On the other hand, low-

energy excitation in heavy-fermion systems can also be described within the Fermi-liquid theory using a quasi-particle picture. This Fermi-liquid approach has recently been applied to CeNiSn by Ikeda and Miyake [21]. They have successfully explained the various anomalous properties at ambient pressure. In their theory, the pseudogap formation at the Fermi level is attributed to the anisotropic hybridization of the quasi-particle and conduction bands. The inelastic-excitation peaks in neutron scattering are also described as particle–hole excitations across the hybridization gap. The hybridization will become larger under pressure because of the reduction of the lattice constant. Thus within the hybridization-gap picture, the width of the hybridization gap, and thus the inelastic-excitation energy $\hbar\omega_0$, will increase under pressure. This is consistent with our experimental results shown in figure 4(a). We note that the pseudogap width, deduced from the electrical resistivity, decreases under pressure, which is opposite to the case for $\hbar\omega_0$. This behaviour may originate from the fact that the resistivity is rather affected by the density of states in the vicinity of the Fermi level. Thus the bottom of the hybridization gap, which will appear as a pseudogap in the resistivity, may collapse under pressure, while the width of the hybridization gap becomes large. As described above, the Fermi-liquid approach can qualitatively explain the behaviour of the inelastic-excitation peak in CeNiSn under high pressure. A quantitative calculation of the density of states under high pressure is highly desired for a conclusive understanding of the different behaviours of the resistivity and neutron scattering.

4. Summary

Neutron inelastic-excitation spectra of CeNiSn under hydrostatic pressure up to 11 kbar were reported. The 4 meV peak of the antiferromagnetic correlation, observed at ambient pressure, shifts to a higher-energy region and its intensity becomes smaller with increasing pressure. This pressure dependence of the intensity indicates that the antiferromagnetic correlation is suppressed under high pressure. Since the pseudogap in the resistivity also collapses under pressure, this result strongly suggests that the antiferromagnetic correlation has a close relationship with the pseudogap formation. The position of the inelastic-excitation peak shifts to a higher-energy region, while the pseudogap width, deduced from the electrical resistivity, becomes smaller, suggesting that they seem to reflect the density of states in different energy regions.

Acknowledgments

The authors thank A Onodera, M Nishi, H Kawada and Y Fujii for technical advice on using the high-pressure cell for neutron scattering. They also thank K Miyake, H Ikeda, Y Okayama, G Nakamoto, L P Regnault and H Yoshizawa for valuable discussions. One of the authors (TT) thanks the Yamada Science Foundation for financial support.

References

[1] Takabatake T, Nakazawa Y and Ishikawa M 1987 *Japan. J. Appl. Phys. Suppl.* 3 **26** 547
Takabatake T and Fujii H 1993 *Japan. J. Appl. Phys.* **8** 254
Takabatake T, Nakamoto G, Tanaka H, Bando Y, Fujii H, Nishigori S, Goshima H, Suzuki T, Fujita T, Oguro I, Hiraoka T and Malik S K 1994 *Physica* B **199+200** 457
[2] Malik S K and Adroja D T 1991 *Phys. Rev.* B **43** 6277
[3] Hundley M F, Canfield P C, Thompson J D, Fisk Z and Lawrence J M 1990 *Phys. Rev.* B **42** 6842
Bucher B, Schlesinger Z, Canfield P C and Fisk Z 1994 *Phys. Rev. Lett.* **72** 522

[4] Allen J W, Batlogg B and Wachter P 1979 *Phys. Rev.* B **20** 4807
[5] Kasaya M, Iga F, Takigawa M and Kasuya T 1985 *J. Magn. Magn. Mater.* **47+48** 429
[6] Higashi I, Kobayashi K, Takabatake T and Kasaya M 1993 *J. Alloys Compounds* **193** 300
[7] Nishigori S, Goshima H, Suzuki T, Fujita T, Nakamoto G, Takabatake T, Fujii H and Sakurai J 1993 *Physica* B **186–188** 406
[8] Nakamura K, Kitaoka Y, Asayama K, Takabatake T, Nakamoto G, Tanaka H and Fujii H 1996 *Phys. Rev.* B **53** 6385
[9] Takabatake T, Nakamoto G, Yoshino T, Fujii H, Izawa K, Nishigori S, Goshima H, Suzuki T, Fujita T, Maezawa K, Hiraoka T, Okayama Y, Oguro I, Menovsky A A, Neumaier K, Brückl A and Andres K 1996 *Physica* B at press
[10] Nakamoto G, Takabatake T, Bando Y, Fujii H, Izawa K, Suzuki T, Fujita T, Minami A, Oguro I, Tai L T and Menovsky A A 1995 *Physica* B **206–207** 840
Nakamoto G, Takabatake T, Fujii H, Minami A, Maezawa K, Oguro I and Menovsky A A 1995 *J. Phys. Soc. Japan* **64** 4834
[11] Mason T E, Aeppli G, Ramirez A P, Clausen K N, Broholm C, Stücheli N, Bucher E and Palstra T T M 1992 *Phys. Rev. Lett.* **69** 490
[12] Kadowaki H, Sato T, Yoshizawa H, Ekino T, Takabatake T, Fujii H, Regnault L P and Isikawa Y 1994 *J. Phys. Soc. Japan* **63** 2074
Sato T J, Kadowaki H, Yoshizawa H, Ekino T, Takabatake T, Fujii H, Regnault L P and Isikawa Y 1995 *J. Phys.: Condens. Matter* **7** 8009
[13] Takabatake T, Nakamoto G, Tanaka H, Bando Y, Fujii H, Nishigori S, Goshima H, Suzuki T, Fujita T, Oguro I, Hiraoka T and Malik S K 1994 *Physica* B **199+200** 457
[14] Sato T J, Kadowaki H, Yoshizawa H, Nakamoto G, Ekino T, Takabatake T, Fujii H, Regnault L P and Isikawa Y 1996 *Physica* B at press
Sato T J, Kadowaki H, Yoshizawa H, Takabatake T, Fujii H and Isikawa Y 1996 *J. Phys.: Condens. Matter* **8** 7127
[15] Raymond S, Regnault L P, Sato T J, Kadowaki H, Nakamoto G, Takabatake T, Fujii H, Isikawa Y and Flouquet J 1996 *J. Phys.: Condens. Matter* submitted
[16] Kurisu M, Takabatake T and Fujiwara H 1988 *Solid State Commun.* **68** 595
Kurisu M, Takabatake T and Fujii H 1994 *Proc. Hiroshima Workshop on Transport and Thermal Properties of f-electron Systems* ed H Fujii, T Fujita and G Oomi (New York: Plenum)
[17] Hiraoka T, Kinoshita E, Takabatake T, Tanaka H and Fujii H 1994 *Physica* B **199+200** 440
[18] Isikawa Y, Mori K, Ogisi Y, Oyaba K and Sato K 1991 *J. Phys. Soc. Japan* **60** 2514
[19] Onodera A, Nakai Y, Kunitomi N, Pringle O A, Smith H G, Nicklow R M, Moon R M, Amita F, Yamamoto N, Kawano S, Achiwa N and Endo Y 1987 *Japan. J. Appl. Phys.* **26** 152
[20] Chesser N J and Axe J D 1973 *Acta Crystallogr.* A **29** 160
[21] Ikeda H and Miyake K 1996 *J. Phys. Soc. Japan* **65** 1769